RNA editing enzyme ADAR1 controls miR-381-3p-mediated expression of multidrug resistance protein MRP4 via regulation of circRNA in human renal cells

Yuji Omata, Maseri Okawa, Mai Haraguchi, Akito Tsuruta,
Naoya Matsunaga, Satoru Koyanagi, Shigehiro Ohdo

Supporting Information

EXPERIMENTAL PROCEDURES

Supplementary Table S1
Primer sets for quantitative RT-PCR analysis for circRNA expression.

Supplementary Figure S1
Effects of the knockdown of ADAR1 on the transcription activity of the *ABCC4* gene.

Supplementary Figure S2
Electropherograms from direct sequencing of the PCR-amplified product of *ABCC4* 3′ UTR.

Supplementary Figure S3
Effect of the knockdown of ADAR1 on the expression levels of circRNAs highly expressed in RPTECs.

Supplementary Figure S4
Estimation the effects of ADAR1-mediated A-to-I RNA editing on the secondary structure of the precursor of circHIPK3.

EXPERIMENTAL PROCEDURES

Direct sequencing

RNA was extracted from RPTECs using the ReliaPrep RNA Cell Miniprep system (Promega) and treated with DNase I on columns. A total of 500 ng of RNA was used for cDNA synthesis with ReverTra Ace qPCR RT Kit (TOYOBO Co., Ltd.). Genomic DNA was extracted using the Wizard Genomic DNA Purification Kit (Promega). The cDNA and genomic DNA were amplified by the GoTaq Green Master Mix (Promega) with the same gene-specific primers used in plasmid construction (Human *ABCC4* 3′UTR; **Table 2**). The PCR-amplified products were analyzed by Sanger sequencing using the same primer used in the PCR (*ABCC4* 3′UTR Reverse for +1741 bp; **Table 2**). Electropherograms were aligned using SnapGene Viewer.

Table S1 Primer sets for quantitative RT-PCR analysis of gene expression

circRNA	Primers
hsa_ZNF124_0005	
Forward	5′-TAAGCAATAAGAACTCGGTTGCC-3′
Reverse	5′-GGGAAGGATCCAACAAAGCCC-3′
hsa-RBM33_0009	
Forward	5′-CCCAGAAGAAGGACAGTATGAA-3′
Reverse	5′-TGTAACACCCTGAGAACTGAAAT-3′
hsa-CGNL1_0010	
Forward	5′-GGGAGCCCTGAAAGAAGAGGT-3′
Reverse	5′-TGGAATTACAAGCCTTGGTTGCT-3′
hsa-ZKSCAN1_0001	
Forward	5′-GAAACCCCGCCTCTTACA-3′
Reverse	5′-TTCCTCTTCCACCTTCACTATTA-3′
hsa-CDYL_0005	
Forward	5′-CTTAGCTGTTAACGGGAAA-3′
Reverse	5′-CTGTTGAAGTCGTGGATGT-3′
hsa-MAN1A2_0003	
Forward	5′-TCTGTGTTTGAAGTCAACATTCG-3′
Reverse	5′-GCTTCTTCCAAGGCCTTCTC-3′
hsa-C3_0002	
Forward	5′-CGGACAAGAAAGGTAACCTGGA-3′
Reverse	5′-AAGTCCTCAACGTTCCACAGC-3′
hsa-FBXW7_0005	
Forward	5′-AGTATTGTGGACCTGCCCGTTC-3′
Reverse	5′-GCCAGCTTGCTACTTCTTGGA-3′
hsa-SLC8A1_0015	
Forward	5′-ATCGAAGGGACTGCCAGAGG-3′
Reverse	5′-GGTGAAAGACTTAATCGCCGC-3′
hsa-PCMTD1_0002	
Forward	5′-CTGAAGTTATGGAAGCATTG-3′
Reverse	5′-ATGGCTTCCAATATTGCACTTG-3′
hsa-PSD3_0018	
Forward	5′-GTCCATTGCCTTACCTGTGCAA-3′
Reverse	5′-TTGGCTGCTTCCACATTGCT-3′
hsa-SMARCA5_0005	
Forward	5′-GAAAAGCTCTCCAAGATGGG-3′
Reverse	5′-CTTCTTTGCACCTCTTTCCAA-3′
hsa-FGGY_0001	
Forward	5′-TCTCCCGGACTTCTTATCGTGG-3′
Reverse	5′-CGATGGTCCAGCCACATGAT-3′
hsa-RHOBTB3_0011	
Forward	5′-AGGCAACCCACCATTACGAG-3′
Reverse	5′-ATGGCTTACAGCGCAGAGAA-3′

hsa-FNDC3B_0004	
Forward	5′-CAAGAAGCAGCCCAAAGTCG-3′
Reverse	5′-CATGGCTGAGGGGTAGCTTG-3′
hsa-ATRNL1_0001	
Forward	5′-CCAATTGCGGCAGTCCAGAT-3′
Reverse	5′-TGGATAGCCTTCAATGAGCCA-3′
hsa-NOX4_0018	
Forward	5′-TCCGGAGCAATAAGCCAGTC-3′
Reverse	5′-TTAAGACTGATGCAGCCGGG-3′
hsa-SETD3_0001	
Forward	5′-AAACACAGCTCGACAGTACGC-3′
Reverse	5′-GCATTTCTGCAGCAGCTCAC-3′
hsa-RAB3IP_0013	
Forward	5′-GTTCTGGAGGCTGTGGAAAA-3′
Reverse	5′-GACACGTCCTGTCCATTGTG-3′
hsa-SLTM_0001	
Forward	5′-AGAGGACATCGAAAGTCAGGAAA-3′
Reverse	5′-TCCACAGAAGCATCTCCACTCA-3′
hsa-MAN1A2_0002	
Forward	5′-GCAAGGAAAGGACACTCCCC-3′
Reverse	5′-TCTTCCTCTTCCCACACTGAAA-3′
hsa-PTK2_0007	
Forward	5′-TTGCCAAAAGGATTTCTAAACCAGT-3′
Reverse	5′-GTTGGGGTCAAGGTAAGCAGC-3′
Human *GAPDH*	
Forward	5′-ACAACTTTGGTATCGTGGAAGG-3′
Reverse	5′-GCCATCACGCCACAGTTTC-3′

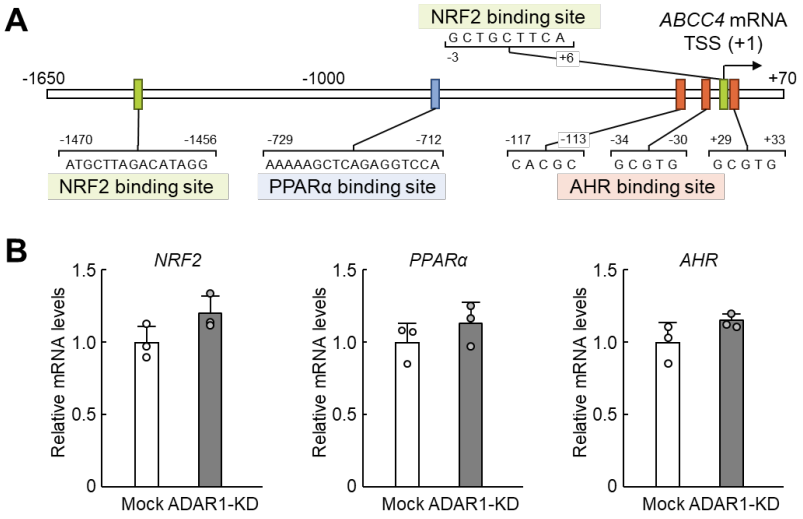

Supplementary Figure S1. Effects of the knockdown of ADAR1 on the transcription activity of the *ABCC4* gene. *A*, schematic diagrams of the 5'-flanking region of the *ABCC4* gene and response elements of well-known transcription factors. The numbers indicate the distance in base pairs from the putative transcription start site (TSS, +1). Binding sites of the transcription factors were searched in JASPAR2022 (https://jaspar.genereg.net/) and referred from a previous study (48). *B*, the mRNA levels of *NRF2*, *PPARα* and *AHR* in mock-transduced and ADAR1-KD RPTECs. The mRNA levels were normalized to those of 18S rRNA. Values are the mean with S.D. (n = 3).

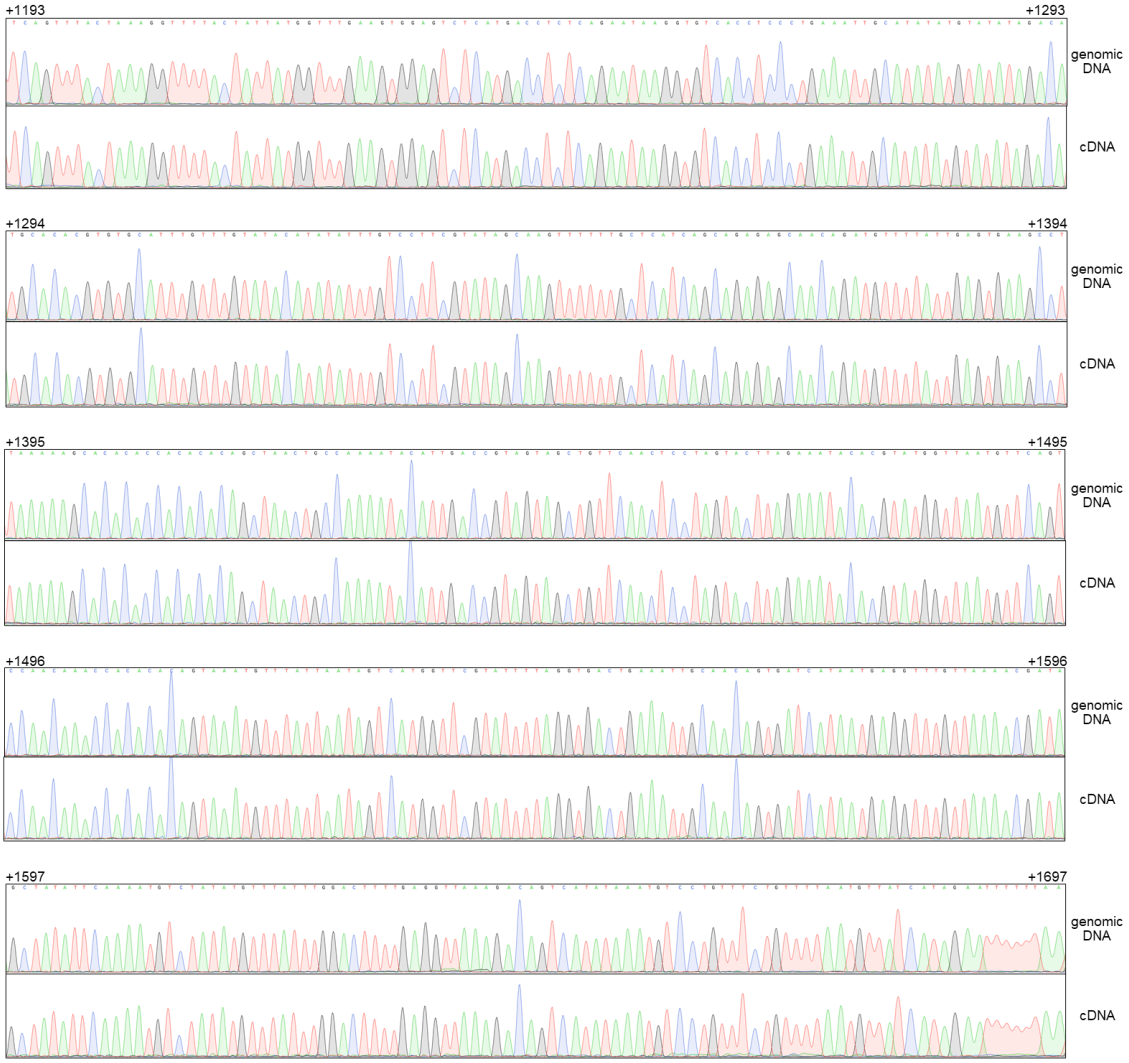

Supplementary Figure S2. Electropherograms from direct sequencing of the PCR-amplified product of *ABCC4* 3′UTR. The sequence data were obtained from genomic DNA and mRNA extracted from RPTECs. The numbers indicate the distance in base pairs from the stop codon (+1). Electropherograms were aligned using SnapGene Viewer.

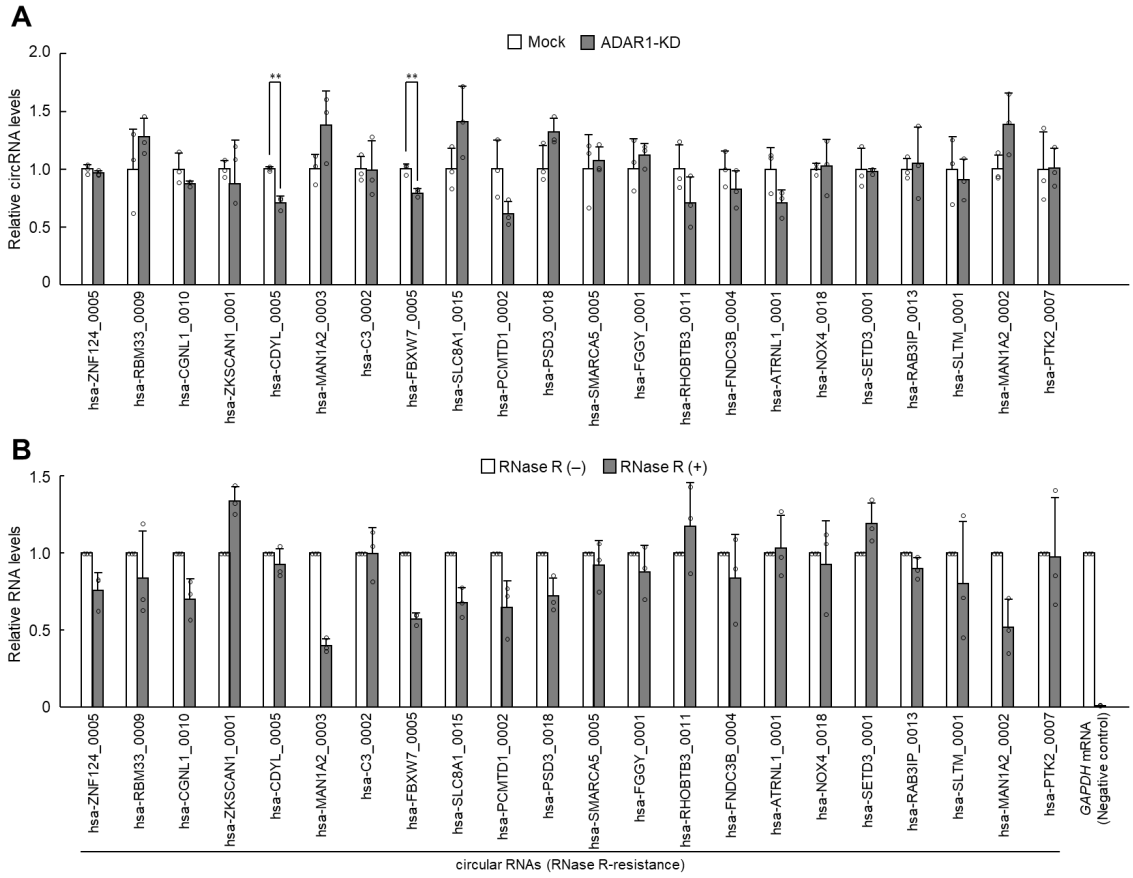

Supplementary Figure S3. Effect of the ADAR1 knockdown on the levels of circRNAs expressed in RPTECs. *A*, the expression levels of circRNAs listed in **Fig. 3A** in mock-transduced and ADAR1-KD RPTECs. The expression levels were normalized to those of 18S rRNA. Values are the mean with S.D. (n = 3). $^{**}p < 0.01$; significant difference between the two groups ($t_4 = 8.067$, $p = 0.001$ for circCDYL; $t_4 = 6.503$, $p = 0.003$ for circFBXW7; unpaired *t*-test, two-sided). *B*, qRT-PCR analysis for the abundance of circRNAs listed in **Fig. 3A** and *GAPDH* mRNA in RPTECs treated with RNase R. The amounts of target RNAs were normalized to those in the mock treatment.

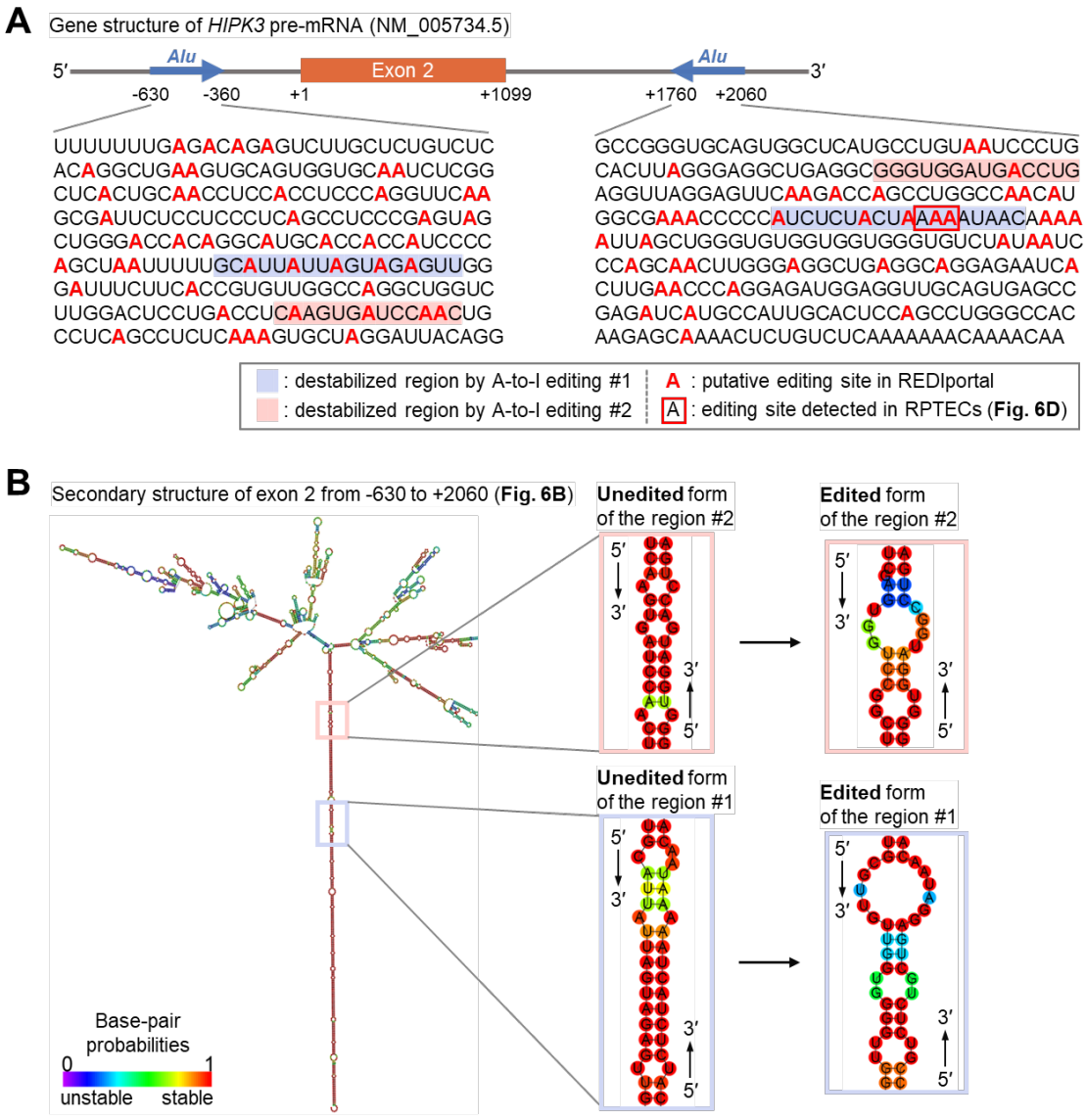

Supplementary Figure S4. Estimation the effects of ADAR1-mediated A-to-I RNA editing on the secondary structure of the precursor of circHIPK3. *A*, schematic diagram of the genomic region of human *HIPK3* exon 2 and its flanking introns with inverted *Alu* elements and detailed sequence of the inverted *Alu* elements. Sequences colored blue or red indicate the putative destabilized regions by A-to-I RNA editing. "A" colored red indicates A-to-I RNA editing sites registered in REDIportal. "A" enclosed in a red square indicates the editing sites detected in RPTECs with direct sequencing. *B*, *in silico* prediction of RNA secondary structure of the putative destabilized regions in precursor of circHIPK3. The *Middle panel* shows the unedited form and the *right panel* shows the edited form of the putative destabilized regions. The minimum free energy structure with base-pair probabilities was calculated to have the lowest value of free energy. Base-pair probabilities are shown by a color spectrum. In the l*eft panel,* the RNA secondary structure of the precursor of circHIPK3 shown in **Fig. 6B** was reused to show the location of the putative destabilized regions by A-to-I RNA editing.